



# Lab on a chip packing of submicron particles for high performance EOF pumping

Qin Lu, Greg E. Collins\*

Naval Research Laboratory, 4555 Overlook Ave., SW Chemistry Division, Code 6112, Washington, DC 20375-5342, USA

## ARTICLE INFO

### Article history:

Received 16 July 2010

Received in revised form 26 August 2010

Accepted 3 September 2010

Available online 15 September 2010

### Keywords:

Packed bed microchannel

EOF pump

Silica beads

High pressure

Lab on a chip

## ABSTRACT

The packing of submicrometer sized silica beads inside a microchannel was enabled by a novel method which avoids the complication and limitations of generating a frit using conventional approaches and the restriction of flow using a submicrometer sized weir. A micrometer sized weir and two short columns of 5  $\mu\text{m}$  and 800 nm silica beads packed in succession behind the weir together functioned as a high pressure frit to allow the construction of a primary packed bed of 390 nm silica beads. This packed bed microchannel was tested as an EOF pump, wherein it exhibited superior performance with regards to pressure tolerance, i.e., sustaining good flow rate under extremely high back pressure, and maximal pressure generation. Under a modest applied electric field strength of 150 V/cm, the flow rate against a back pressure of 1200 psi ( $\sim 8.3$  MPa) was 40 nL/min, and the maximal pressure reached 1470 psi ( $\sim 10$  MPa). This work has demonstrated that it is possible to create a high performance packed bed microchannel EOF pump using nanometer sized silica beads, as long as proper care is taken during the packing process to minimize the undesirable mixing of two different sized particles at the boundaries between particle segments and to maximize the packing density throughout the entire packed bed.

Published by Elsevier B.V.

## 1. Introduction

Electroosmotic flow (EOF) pumps incorporated directly onto planar substrates in a lab on a chip format can be categorized into two basic types: open microchannel EOF pumps and packed bed microchannel EOF pumps. Although open microchannel EOF pumps are capable of transporting fluid with high flow rates in the absence of any back pressure, they are generally not suitable for high pressure applications, due to their low hydraulic resistance associated with the open channel geometry. One exception is a multiple, parallel shallow channel (1–6  $\mu\text{m}$ ) microchip EOF pump which was able to generate flow rates of 10–400 nL/min and a maximal pressure of 80 psi ( $\sim 0.55$  MPa) at an applied electric field strength of 1 kV/cm [1]. On the other hand, it has been demonstrated that EOF pumps utilizing packed capillaries have much better performance in terms of overall output pressure than the open capillary EOF pumps [2–5]. Pressures in excess of 8000 psi ( $\sim 55$  MPa) have been generated utilizing packed capillary EOF pumps [2] and these pumps were attractive in high pressure applications such as the miniaturization of HPLC systems.

Despite the success in generating high pressures with packed capillary EOF pumps, there are only a few reports that detail the development of high pressure EOF pumps using packed bed

microchannels in a microchip format [6–8]. The reasons are multifold. Generating a packed bed inside a microchannel is not a trivial task. The frit preparation methods, such as those most commonly utilized for packed capillaries found in electrochromatography [9–11] are difficult to implement within a microfabricated microchannel on a planar substrate. Furthermore, there are many problems associated with frits, including bubble generation, and the lack of stability in high pressure applications. Instead of using a frit, the microchannel can include a tapered geometry to induce particles to aggregate, whereupon they act as “keystones” for blocking subsequent particles packed behind them [12]. This approach is not suitable for high pressure applications, however. Alternatively, applications requiring a packed bed microchannel with micrometer sized beads for on-chip solid-phase extraction, electrochromatography [13], and immunoassays [14] have utilized true physical barriers in the form of weir structures that are fabricated inside a microchannel to reduce the depth of the microchannel at the weir such that it is smaller than the diameter of the packing beads. This fabrication procedure is straightforward and the resulting weir structure has excellent stability under high pressure conditions. However, if submicrometer or even tens of nanometer sized beads are needed as the packing material, extremely small cross-sectional areas at the weir are necessary in order to retain the small beads. In addition to the difficulties of successfully performing the fabrication of weir structures bearing nanometer scale height differences, EOF flow will be significantly reduced downstream of the weir, a result which is undesirable in most applications.

\* Corresponding author. Tel.: +1 2024043337; fax: +1 2024048119.

E-mail address: [greg.collins@nrl.navy.mil](mailto:greg.collins@nrl.navy.mil) (G.E. Collins).

Report Documentation Page				Form Approved OMB No. 0704-0188	
Public reporting burden for the collection of information is estimated to average 1 hour per response, including the time for reviewing instructions, searching existing data sources, gathering and maintaining the data needed, and completing and reviewing the collection of information. Send comments regarding this burden estimate or any other aspect of this collection of information, including suggestions for reducing this burden, to Washington Headquarters Services, Directorate for Information Operations and Reports, 1215 Jefferson Davis Highway, Suite 1204, Arlington VA 22202-4302. Respondents should be aware that notwithstanding any other provision of law, no person shall be subject to a penalty for failing to comply with a collection of information if it does not display a currently valid OMB control number.					
1. REPORT DATE <b>26 AUG 2010</b>		2. REPORT TYPE		3. DATES COVERED <b>00-00-2010 to 00-00-2010</b>	
4. TITLE AND SUBTITLE <b>Lab on a chip packing of submicron particles for high performance EOF pumping</b>				5a. CONTRACT NUMBER	
				5b. GRANT NUMBER	
				5c. PROGRAM ELEMENT NUMBER	
6. AUTHOR(S)				5d. PROJECT NUMBER	
				5e. TASK NUMBER	
				5f. WORK UNIT NUMBER	
7. PERFORMING ORGANIZATION NAME(S) AND ADDRESS(ES) <b>Naval Research Laboratory, Chemistry Division, Code 6112, 4555 Overlook Ave., SW, Washington, DC, 20375-5342</b>				8. PERFORMING ORGANIZATION REPORT NUMBER	
9. SPONSORING/MONITORING AGENCY NAME(S) AND ADDRESS(ES)				10. SPONSOR/MONITOR'S ACRONYM(S)	
				11. SPONSOR/MONITOR'S REPORT NUMBER(S)	
12. DISTRIBUTION/AVAILABILITY STATEMENT <b>Approved for public release; distribution unlimited</b>					
13. SUPPLEMENTARY NOTES					
14. ABSTRACT <b>The packing of submicrometer sized silica beads inside a microchannel was enabled by a novel method which avoids the complication and limitations of generating a frit using conventional approaches and the restriction of flow using a submicrometer sized weir. A micrometer sized weir and two short columns of 5 m and 800nm silica beads packed in succession behind the weir together functioned as a high pressure frit to allow the construction of a primary packed bed of 390nm silica beads. This packed bed microchannel was tested as an EOF pump, wherein it exhibited superior performance with regards to pressure tolerance, i.e., sustaining good flow rate under extremely high back pressure, and maximal pressure generation. Under a modest applied electric field strength of 150 V/cm, the flow rate against a back pressure of 1200 psi (&amp;#8764;8.3 MPa) was 40 nL/min, and the maximal pressure reached 1470 psi (&amp;#8764;10 MPa). This work has demonstrated that it is possible to create a high performance packed bed microchannel EOF pump using nanometer sized silica beads, as long as proper care is taken during the packing process to minimize the undesirable mixing of two different sized particles at the boundaries between particle segments and to maximize the packing density throughout the entire packed bed.</b>					
15. SUBJECT TERMS					
16. SECURITY CLASSIFICATION OF:			17. LIMITATION OF ABSTRACT <b>Same as Report (SAR)</b>	18. NUMBER OF PAGES <b>5</b>	19a. NAME OF RESPONSIBLE PERSON
a. REPORT <b>unclassified</b>	b. ABSTRACT <b>unclassified</b>	c. THIS PAGE <b>unclassified</b>			

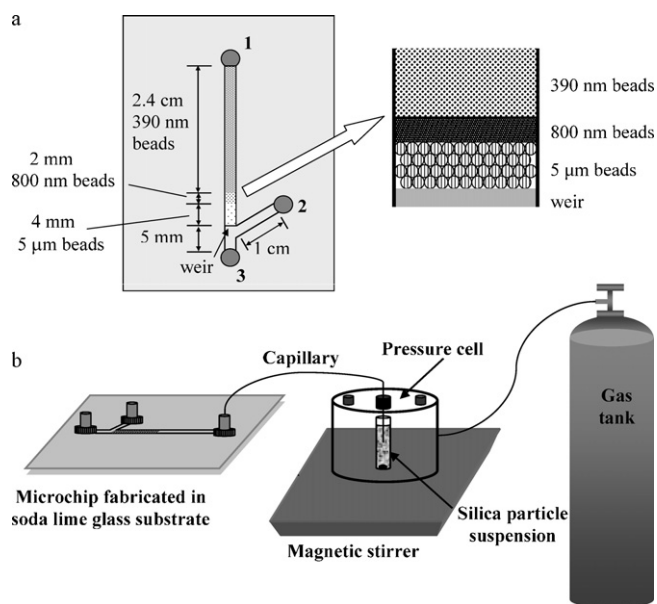


**Fig. 1.** (a) Microchip layout; (b) instrumental setup for packing silica particles inside microchannel.

We report here a novel method which enables the packing of microchannels with submicrometer to tens of nanometer sized particles using a micrometer sized weir as the starting point. The packing methodology discussed here has wide applicability to all lab on a chip techniques that would benefit from the capability for uniformly packing microchannels with beads of smaller and smaller diameters, including EOF pump, electrochromatography, and HPLC on a chip. The quality of the packed bed microchannels reported here, which were comprised of three different sized silica beads in succession of reduced diameter, were evaluated based on their performance as an EOF pump, including the capability for supporting good flow rates against high back pressures under a fixed electric field, the generation of maximum flow rates in the absence of any back pressure, and the generation of maximum pressure at the point of zero net flow as a function of applied electric field.

## 2. Experimental

### 2.1. Reagents

Cyclohexylamino alkyl sulfonate (CHES) was purchased from Sigma-Aldrich (St. Louis, MO). Silica beads (5 μm, 800 nm and 390 nm in diameter) were obtained from Macherey-Nagel (Bethlehem, PA) and Bangs Laboratory (Fisher, IN), respectively. Deionized water was obtained from a Milli-Q Plus (Millipore, Billerica, MA) water system.

### 2.2. Microchip design and fabrication

The microchip design is depicted in Fig. 1(a). It was fabricated by standard photolithography and wet etching techniques, using a soda lime glass substrate coated with chromium and photoresist (Nanofilm, Westlake Village, CA). A weir structure was incorporated in the microchannel to enable packing of the silica particles; this feature requires two separate photolithography and wet etching steps during the microfabrication process. The details of the microchip fabrication can be found elsewhere [8]. The microchannel generated during the first step of photolithography exposure and wet etching had dimensions of 65 μm deep and 100 μm wide at half depth. The second step of photolithography exposure and wet etching created a weir with a depth of ~4.0 μm.

### 2.3. Packed bed generation

The packed bed microchannel was formed by first packing a 0.4 cm length of 5 μm porous silica particles behind the weir structure, followed by a 0.2 cm length of 800 nm silica particles and, finally, a 2.4 cm length of 390 nm silica particles. The length of the 5 μm and 800 nm particle segments were minimized with relation to the 390 nm particles in order to reduce the back pressure driven flow and enhance the performance of the EOF pump under high back pressure conditions. Shown in Fig. 1(a) is the layout of the microchip, indicating the lengths of the different segments of the packed bed on the left side, as well as a close-up view of the relative size of the different packing beads on the right side. The packing length can be controlled by visually monitoring the packing progress with the aid of a microscope and removing the applied pressure at the desired length. It is relatively difficult to keep the column of 5 μm silica particles at 0.2 cm when compared to the 800 nm silica particles (large particles form columns faster), so a length of 0.4 cm was used for the 5 μm particle segment. Using this method, the length of the shorter columns of 5 μm and 800 nm particles were controlled to within 0.1–0.2 mm. This approach enabled the packing of particles with diameters in the hundreds of nanometers to tens of nanometers dimensions without the need for making a frit or fabricating a nano-weir structure. To obtain a densely packed column, a high pressure connection between the microchip inlet access hole and the capillary (360 μm o.d.) output of the packing tool was made possible by using Nanoport assemblies from Upchurch Scientific (Oak Harbor, WA). The capillary was connected to either a syringe whose needle tip had an o.d. of 360 μm, or a pressure cell (Next Advance, Rensselaer, NY). Due to the failure of epoxies to adequately seal the Nanoport assemblies to the glass microchips, the high pressure sealing was provided by a homemade microchip holder [8]. The first two segments of the packed bed were formed by packing 5 μm and 800 nm silica particles using a manual, handheld syringe pump from Unimicro Technologies (Pleasanton, CA) mounted with a plastic syringe filled with a slurry of 2 wt.% silica beads (~0.5 ml). The third segment was formed by packing a stirred slurry of 4 wt.% silica beads (390 nm) using the Next Advance pressure cell connected to an argon tank (Fig. 1(b)). The backend of the packed bed was left unsealed to avoid problems associated with frits, such as bubble formation. The diameters of the particles utilized for the three different segments were not optimized, although the pore radius of each particle was accounted for to ensure each preceding segment was a true barrier for the following segment. As a measure of column integrity, application of 1500 psi pressure from an argon tank to the column in the direction of front-end to back-end left the column visually intact.

### 2.4. Packed bed evaluation

Evaluation of the quality of the packed bed was performed by investigating its performance as an EOF pump. Studies included measurements of (a) the net flow rates against a range of high back pressures under a fixed electric field, (b) the maximum flow rate in the absence of any back pressure, and (c) the maximum pressure generated at the point of zero net flow as a function of applied electric field. The pump fluid used for all of the measurements was aqueous CHES buffer (10 mM, pH 9.0). At least three measurements were performed for each data point. Reproducibility from run-to-run and device to device was good, with standard deviations less than 7%. The technique used to measure the flow rate was based on tracking the liquid/air meniscus with the aid of a Zeiss Stereomicroscope (Thornwood, NY) within a 100 μm i.d. fused silica capillary that was connected to the field-free outlet, reservoir 3 (Fig. 1(a)). The measured meniscus velocity and the capillary cross-sectional area were used to compute the flow rate. The flow rate against a

back pressure was determined, similarly. The microchip field-free outlet reservoir 3 was connected to a pressure cell via a 50 cm long capillary (100  $\mu\text{m}$  i.d.). The back pressure was applied to the pressure cell using an argon gas tank. Although evaporation of the liquid at the liquid air meniscus is unavoidable, we estimate this will give only a minor error, with the reported flow rate values erring on the low side. Maximum pressure determinations were measured by connecting a 25  $\mu\text{m}$  id fused silica capillary to the field-free outlet reservoir 3. The capillary was 30 cm in length, having the far end sealed with epoxy. The volume of air trapped within the capillary before ( $V_0$ ) and after ( $V_1$ ) the application of an electric field across the packed bed microchannel (between reservoir 1 and reservoir 2) was measured by tracking the motion of the liquid/air meniscus until it reached an equilibrium position. The resulting pressure ( $P$ ) was estimated using Boyle's law:  $P_1 = P_0 V_0 / V_1$ . The electric field strength was maintained  $\leq 150$  V/cm in order to avoid cracking of the microchannel, as was observed previously for these soda lime glass microchips [8].

Images of the three segments of different sized particles contained within the packed beds were taken using an Olympus CKX41 microscope (Center Valley, PA). The scanning electron microscope (SEM) image of a cross-sectional view of the 390 nm silica particles packed inside a microchannel was obtained using a LEO SEM (Carl Zeiss SMT Inc., Peabody, MA). The microchannel was cut at an arbitrary location of the packed bed of 390 nm particles with a Diamond Laser Band Saw (Tampa, Florida).

In order to monitor the overall stability of the different packed beds, the extent of Joule heating, and the adverse impact of gas production due to electrolysis at the surface of the electrodes, electric current through the two electrodes was recorded and monitored continually during the measurements by connecting a digital electrometer (Keithley, Cleveland, OH) in series with the grounded electrode. The current was stable during the time frame of the measurements ( $<10$   $\mu\text{A}$  at an applied field strength of 500 V/cm), and was linearly proportional to the applied electric field strength ( $R^2 > 0.99$ ), indicating minimal problems associated with Joule heating. The pump fluid in the inlet and ground reservoirs was replenished from time to time in order to minimize variations in pH and buffer concentration. These experiments were performed with the waste reservoir 3 open to prevent any buildup of pressure that might physically damage the chip.

### 3. Results and discussion

#### 3.1. Theoretical background

Zeng et al. [5] have defined in Eq. (1) the flow rate for a fluid electroosmotically pumped through a packed capillary filled with porous media under a pressure gradient, assuming that the double layer thickness is smaller than 2% of the mean pore radius,  $a$ .

$$Q = \frac{\psi \Delta P A a^2}{8 L \eta \tau} - \frac{\psi \epsilon \zeta V A}{L \eta \tau} \quad (1)$$

The flow rate,  $Q$ , is governed by several parameters which can be sorted into four groups: (1) the driving forces: electric field,  $V$ , and pressure difference (downstream minus upstream) along the length of the capillary,  $\Delta P$ ; (2) the properties of a packed capillary: length,  $L$ , cross-sectional area,  $A$ , tortuosity,  $\tau$ , porosity,  $\psi$ , and pore radius of the packed bed,  $a$ ; (3) the properties of the pump fluid: permittivity,  $\epsilon$ , and viscosity,  $\eta$ ; and (4) the properties of the electrical double layer near the microchannel wall and the surface of the silica particles: zeta potential,  $\zeta$ , which is affected by the pump fluid used.

Despite the fact that Eq. (1) was derived for a packed capillary, it provides important insights into understanding the behavior of a packed bed microchannel EOF pump. We know from Eq. (1) that

both EOF and pressure-driven flows are proportional to the porosity and the cross-sectional area of the packed bed microchannel, and inversely proportional to the tortuosity of the packed bed and the viscosity of the pump fluid. EOF is proportional to the applied electric field strength, zeta potential, and permittivity of the pump fluid filling the packed bed, and the pressure-driven flow is proportional to the pressure gradient and the pore radius of the packed bed squared.

The maximum flow rate ( $\Delta P = 0$ ) and the maximum pressure ( $Q = 0$ ) of a packed bed microchannel EOF pump, taking into account the applied electric field, the properties of the packed bed microchannel, the properties of the pump fluid, and the zeta potential, can be derived from Eq. (1):

$$Q_{\max} = \frac{\psi \epsilon \zeta V A}{L \eta \tau} \quad (2)$$

$$\Delta P_{\max} = \frac{8 \epsilon \zeta V}{a^2} \quad (3)$$

For most microfluidic applications, reasonable flow rate generation under a back pressure ( $\Delta P > 0$ ) condition is one of the most critical parameters of packed bed microchip EOF pumps, particularly when these pumps are used to drive a mobile phase through an integrated downstream packed bed stationary phase such as that found in  $\mu$ -HPLC. As such, the most important factor for boosting the pressure tolerance of packed bed microchannel EOF pumps is the pore radius of the packed bed, which has an inverse square dependence to the maximum pressure (Eq. (3)), and can be easily reduced by using silica beads of smaller diameter.

#### 3.2. The stability of the packed bed microchannel

In order to avoid the limitations and difficulties associated with implementing a frit within a microchannel for supporting a packed bed, a weir structure was fabricated instead to anchor the packed bed. However, because submicrometer sized beads (390 nm diameter) were the desired packing material, an extremely small cross-sectional area weir would normally be required to retain the small particles. A weir which is  $\sim 300$ – $350$  nm in size is both difficult to microfabricate and results in a significant reduction in EOF downstream of the weir. To overcome these limitations, we developed a novel method for retaining such small beads that begins with the fabrication of a micrometer sized weir ( $\sim 4$   $\mu\text{m}$ ) which is simple to microfabricate and results in less restriction of flow (see Fig. 1(a)). This weir is used to retain a short column of silica beads with diameter slightly larger than the depth of the weir (5  $\mu\text{m}$  diameter), and this short column in turn acts as a frit to retain smaller silica beads (800 nm diameter) packed behind this short column, and so forth, leading to the packing of the primary column of the smallest silica particles (390 nm diameter). The rationale behind this approach is that, in theory, the packed bed porosity,  $\psi$ , and, therefore, the tortuosity,  $\tau$ , are independent of the particle size in a perfectly packed bed. The first two segments (short columns of 5  $\mu\text{m}$  and 800 nm silica beads) in combination with the weir enable the construction of what might be considered a "frit" that is mechanically strong, bears high pressure tolerance, and has the same  $\zeta$  potential as the major portion of the packed bed that is comprised of 390 nm silica beads.

Stability and optimal performance of this type of three-tiered packed bed inside a trapezoidal shaped microchannel is dependent upon the realization of a high quality packed bed wherein care is taken to (1) minimize the undesirable mix of two different sized particles at the boundaries between sections of 5  $\mu\text{m}$ , 800 nm, and 390 nm particles, and (2) maximize the packing density throughout the entire packed bed. The former can be achieved by removing any residual beads from reservoir 1 that are leftover from the pre-



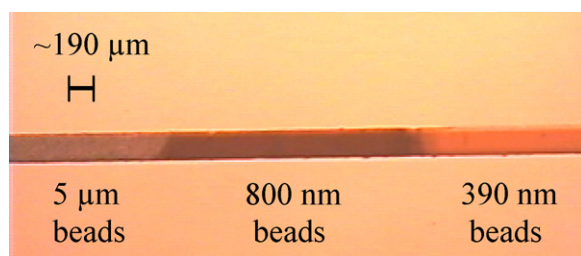


**Fig. 2.** Microscopic images of a portion of a uniformly packed bed showing all three segments with the different sized beads under an applied electric field strength of 1 kV/cm.

vious segment before introducing the beads for packing the next segment. The latter can be accomplished by (1) applying a back flow intermittently during the packing of 5  $\mu\text{m}$  beads to force them to settle into a denser packing, especially in the corners of the microchannel and in the regions near the microchannel wall; (2) maintaining a good slurry suspension during the packing of 390 nm silica beads using a magnetic stir bar (Fig. 1(b)); and (3) shortening the packing time by using high pressure (1200 psi) and 4 wt.% slurry of 390 nm silica beads. A 3-cm long packed bed could be created within 4 h by using the procedure described in Section 2.3 and the detailed points described above. Fig. 2 shows a microscope image taken of a high quality packed bed microchannel with an electric field strength of 1 kV/cm applied across the packed bed. Fig. 3 is an SEM image of a cross-sectional view of the 390 nm particles packed inside the microchannel, obtained by cutting the microchannel using a diamond saw. This figure demonstrates that the space near the microchannel wall was densely packed without sizable voids. The stability of this packed bed was verified via the absence of two problems under prolonged application of electric field ( $E \geq 500 \text{ V/cm}$ ) that plagued our early attempts to create packed beds: bubble formation and packed bed fragmentation. Bubble formation refers to the generation of bubbles within the packed bed and fragmentation refers to the rupture of the packed bed accompanied, in some cases, by the exit of portions of the ruptured packed bed through the unsealed backend in a direction opposite to the EOF flow.

Bubble formation and fragmentation result in a non-functional packed bed, but can be avoided by using the packing procedure described above. Rathore and Horváth [15] discuss the presence

of axial nonuniformities that exist in a typical CEC column in the transition from a packed bed to an open segment and the impact these nonuniformities have upon performance. Nonuniformities also existed in the packed bed microchannels generated in our early attempts to pack tiered particle segments, due to (1) an unwanted mix of two different sized particles at the boundaries between sections of 5  $\mu\text{m}$ , 800 nm, and 390 nm particles, (2) a lower packing density near the microchannel wall and at the corners of the trapezoidal microchannel, especially in the 5  $\mu\text{m}$  particle segment due to a lower channel-to-particle size ratio, and (3) disparity in packing density that existed in the 390 nm particle segment due to the existence of regions of “bad packing,” or regions of differing packing density.

As a result of the conservation of mass which requires that the volumetric flow rate of the pump fluid be the same across the entire packed bed, a local pressure,  $P_i$ , develops at the boundaries between sections of different packing densities within the packed bed. This local pressure,  $P_i$ , can be higher or lower than that at the inlet and outlet of the microchannel,  $P_0$ , and it is this pressure difference that provides a mechanism to support a uniform volumetric flow rate throughout the entire packed bed. Bubble formation and fragmentation of a poorly packed bed may be explained by the presence of this local pressure,  $P_i$ . In the case of bubble formation, for example, as the applied electric field reaches a certain threshold, a local pressure,  $P_i$ , much lower than the atmospheric pressure,  $P_0$ , develops within the packed bed, causing degassing and even the vaporization of the pump fluid. In the case of packed bed fragmentation, a much higher local pressure,  $P_i$ , develops within the packed bed. The flow driven by this local high pressure is in the direction both with and against EOF, ultimately causing the rupture of the packed bed. The flow against the EOF together with the electrophoretic migration of the negatively charged broken segments eventually results in the exit of the broken segments out of the microchannel through its unsealed backend. These two types of local pressures,  $P_i < P_0$  and  $P_i > P_0$ , coexist when an electric field is applied across the entire packed bed. The observed result is the dominant event triggered by the biggest change in local pressure with respect to the atmospheric pressure.

### 3.3. The performance of the packed bed microchannel as EOF pump

A packed bed microchannel could be reproducibly generated, devoid of any failings associated with bubble formation and fragmentation, by using the method described above. After confirming the stability of the packed bed microchannel under a prolonged application of electric field at  $E > 500 \text{ V/cm}$ , its performance as an EOF pump was evaluated via its capability for sustaining good flow rate under high back pressure conditions, and by determining the maximum flow rate and pressure achievable under a modest electric field strength of 150 V/cm.

The net flow rates were determined using the method described in Section 2.4, applying a range of back pressures to the field free reservoir 3 while an electric field strength of 150 V/cm was applied between reservoir 1 and reservoir 2 (see Fig. 1(a) for microchip configuration). As expected from Eq. (1), the higher the back pressure, the lower the net flow rate (Fig. 4(a)), due to an increase in the pressure driven flow in the opposite direction to that of the EOF. Because the majority length of the packed bed microchannel is composed of 390 nm particles, the small pore radius within the packed bed generates a very high hydraulic resistance to counter the pressure driven flow opposed to the EOF. As a result, at back pressures as high as 1200 psi ( $\sim 8.3 \text{ MPa}$ ), this packed bed microchannel EOF pump was still able to maintain a flow rate of 40 nL/min, even if the applied electric field strength was only at 150 V/cm.

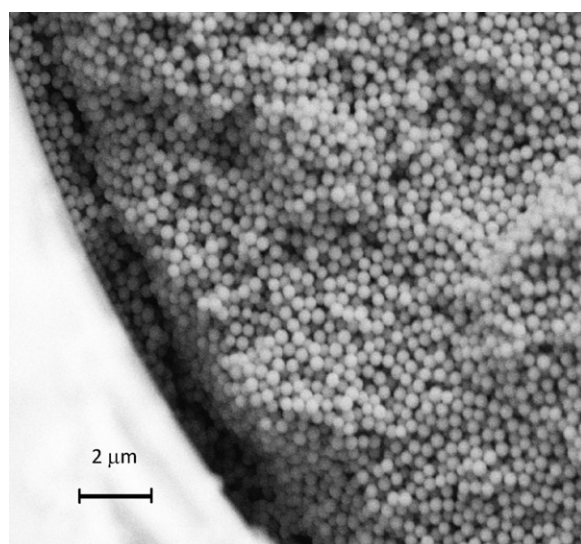


**Fig. 3.** SEM image of the cross-sectional view of 390 nm particles packed inside the microchannel.

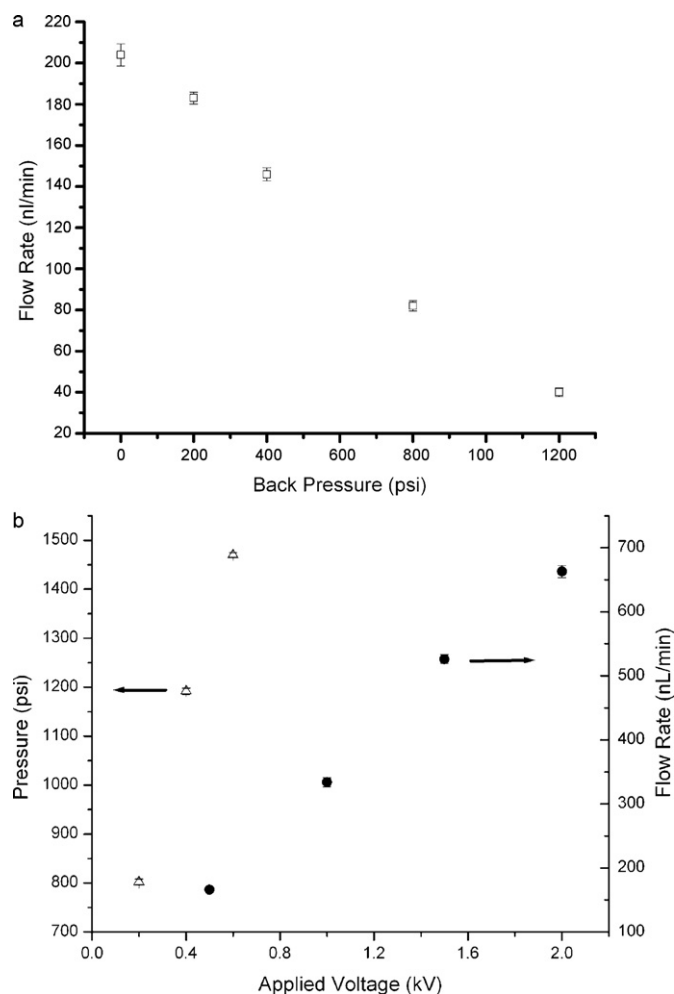


**Fig. 4.** (a) Flow rate,  $Q$ , versus the applied backpressure,  $\Delta P$ , under applied electric field strength of 150 V/cm. (b) Maximum flow rate,  $Q_{max}$ , and maximum pressure,  $\Delta P_{max}$ , versus the applied voltage: open triangle =  $\Delta P_{max}$ ; closed circle =  $Q_{max}$ .

The  $Q_{max}$  and  $\Delta P_{max}$  generated by the packed bed microchannel EOF pump were determined and the results are plotted in Fig. 4(b). From Eq. (2), it is recognized that at a fixed electric field strength,  $Q_{max}$  is independent of the particle size, as long as the properties of the packed bed microchannel remain unchanged, such as cross-sectional area,  $A$ , tortuosity,  $\tau$ , and porosity,  $\psi$ , and as long as the bead diameter is greater than  $0.2 \mu\text{m}$  [16]. Indeed, under the same electric field strength, the maximum flow rates generated by this packed bed microchannel EOF pump when packed with 390 nm silica beads was similar to those generated by a previously reported packed bed microchannel EOF pump with 800 nm sized particles [8], in which both microchannels and weir structures had similar dimensions. Because  $\Delta P_{max}$  is inversely proportional to the square of the pore radius,  $a$  (see Eq. (3)), and the packed bed microchannel EOF pump using 390 nm silica beads comprises smaller pores, it generated an unprecedented high pressure (1470 psi,  $\sim 10 \text{ MPa}$ ) at the modest electric field strength of 150 V/cm (the highest pressure

generated to date by a microchip EOF pump was 1000 psi ( $\sim 7 \text{ MPa}$ ) at the electric field strength of 200 V/cm [8]). Even more impressive is the realization that the packed bed maintained its integrity under such a high pressure, despite the absence of a backend frit.

#### 4. Conclusions

A novel method has been developed to enable the packing of submicrometer, even possibly tens of nanometer-sized beads in a microchannel using a micrometer sized weir structure. Silica beads with diameter slightly larger than the depth of the weir are packed immediately after the weir to form a short column that acts as a frit to retain smaller silica beads packed behind this short column. Based on the same principle, a packed bed inside a microchannel has been constructed using three different sized silica beads in order of decreasing diameter, with the major portion of the packed bed composed of 390 nm silica beads. Our results demonstrate that this approach can be utilized to create high quality packed bed microchannels exhibiting superior performance as EOF pumps. Under a modest electric field strength, 150 V/cm, this packed bed microchannel EOF pump generated a pressure as high as 1470 psi ( $\sim 10 \text{ MPa}$ ) and supported a flow rate of 40 nL/min under 1200 psi ( $\sim 8.3 \text{ MPa}$ ) back pressure. We believe this method is very useful for packing submicrometer, even possibly tens of nanometer sized particles in a microchannel where the fabrication of a high quality frit is hard to achieve, and has great impact on applications in which electric field is the driving force for flow generation under high back pressure, such as EOF pump integrated with a reverse phase stationary phase for chromatography on a single planar microchip.

#### Acknowledgement

The authors would like to thank the Office of Naval Research (ONR) for funding support of this effort through the Naval Research Laboratory (NRL).

#### References

- [1] I.M. Lazar, B.L. Karger, *Anal. Chem.* 74 (2002) 6259.
- [2] P.H. Paul, D.W. Arnold, D.J. Rakestraw, in: D.J. Harrison, A. van den Berg (Eds.), *Micro Total Analysis Systems*, Kluwer Academic Publishers, Boston, MA, 1998, p. 49.
- [3] P.H. Paul, D.W. Arnold, D.W. Neyer, K.B. Smith, in: A. van den Berg, W. Olthuis, P. Bergveld (Eds.), *Micro Total Analysis Systems*, Kluwer Academic Publishers, Boston, MA, 2000, p. 583.
- [4] L. Chen, Y. Guan, J. Ma, G. Luo, K. Liu, *J. Chromatogr. A* 1064 (2005) 19.
- [5] S. Zeng, C.-H. Chen, J.C. Mikkelsen Jr., J.G. Santiago, *Sens. Actuatur. B* 79 (2001) 107.
- [6] T.T. Razunguzwa, A.T. Timperman, *Anal. Chem.* 76 (2004) 1336.
- [7] J. Borowsky, Q. Lu, G.E. Collins, *Sens. Actuatur. B* 131 (2008) 333.
- [8] Q. Lu, G.E. Collins, *Lab. Chip* 9 (2009) 954.
- [9] R.T. Kennedy, J.W. Jorgenson, *Anal. Chem.* 61 (1989) 1128.
- [10] N.W. Smith, M.B. Evans, *Chromatographia* 38 (1994) 649.
- [11] R.J. Boughtflower, T. Underwood, C.J. Paterson, *Chromatographia* 40 (1995) 329.
- [12] L. Ceriotti, N.F. de Rooij, E. Verpoorte, *Anal. Chem.* 74 (2002) 639.
- [13] R.D. Oleschuk, L.L. Shultz-Lockyear, Y. Ning, D.J. Harrison, *Anal. Chem.* 72 (2000) 585.
- [14] K. Sato, M. Tokeshi, T. Odake, H. Kimura, T. Ooi, M. Nakao, T. Kitamori, *Anal. Chem.* 72 (2000) 1144.
- [15] A.S. Rathore, Cs. Horváth, *Anal. Chem.* 70 (1998) 3069.
- [16] Th. Adam, S. Lüdtkke, K.K. Unger, *Chromatographia* 49 (1999) S49.